Effects of film thickness on manganite film-based heterjunctions

W. M. Lü, A. D. Wei, J. R. Sun,[a] Y. Z. Chen, and B. G. Shen
Beijing National Laboratory for Condensed Matter Physics and Institute of Physics, Chinese Academy of Sciences, Beijing 100080, People's Republic of China

(Received 29 December 2008; accepted 6 February 2009; published online 25 February 2009)

Effects of film thickness on interfacial barrier have been studied for the $La_{0.67}Ca_{0.33}MnO_3/SrTiO_3:Nb$ and $La_{0.67}Sr_{0.33}MnO_3/SrTiO_3:Nb$ junctions. In addition to the evolution of the transport behavior from electron tunneling to thermionic emission, increase in film thickness from ~5 to ~50 nm causes a significant growth of interfacial barrier as revealed by photoresponse experiments, and the maximum change in interfacial barrier is ~13% for $La_{0.67}Ca_{0.33}MnO_3/SrTiO_3:Nb$ and ~45% for $La_{0.67}Sr_{0.33}MnO_3/SrTiO_3:Nb$. A linear relation between interfacial barrier and lattice constant of the films is further found, which suggests the influence of lattice strains on interfacial barrier. Qualitative explanations are given. © *2009 American Institute of Physics*. [DOI: 10.1063/1.3089698]

Manganite junctions have received significant attention in recent years because of their attractive properties. In addition to rectifying,[1,2] they own a lot of extraordinary properties such as strongly bias-dependent magnetoresistance[2,3] and temperature/magnetic field-dependent photovoltaic effect.[4] In the scenario of the buildup of interfacial potential, due to the different Fermi energies of manganites and, for example, $SrTiO_3:Nb$, which constructs the most intensively studied Schottky junctions, and the variation of this potential under external disturbances, these behaviors can be understood qualitatively.

We found that the junctions previously investigated are constructed by manganite films thicker than 100 nm. However, the important artificial materials, which are expected to be the focus of future study, are usually composed of layers several nanometers in thickness, a scale required to activate interlayer coupling. Furthermore, the interface/size effect, which emerges and develops as film thickness (t) decreases, has its special meanings as far as manganites being concerned. As well known, a distinctive feature of the manganite is the strong coupling between spin/charge/orbital degrees of freedom and lattice strains.[5] The crucial role of the latter has been experimentally demonstrated. For example, lattice-strain-modulated spin/orbital ordering has been observed in the $La_{1-x}Sr_xMnO_3$ films;[6] it is also found that a great anisotropic conduction can be realized simply by tuning lattice strains.[7] However, to what degree the rectifying property of the junction retains as film thickness decreases and what is the effect of surface/interface and lattice strain have not been addressed. These are important issues noting the general tendency for the electronic devices/materials toward nanometer scales. The thorough knowledge in this regard will benefit not only to the understanding of the diverse behaviors of the heterostructure/junction but also to the designing of artificial materials. Based on these considerations, in this letter we will perform a systematic study of the effect of film thickness on manganite junctions. Special attention has been paid to the variation in the Schottky barrier with film thickness. Photovoltaic technique has been used here to avoid the difficulties encountered by the analyses of the current (I)–voltage (V) and capacitance-voltage relations, especially for ultrathin films, for which electron tunneling prevails. A strong dependence of interfacial barrier on film thickness is observed; the former grows significantly with the latter. The tensile strain in the films is further proven to be the key factor affecting interfacial barrier.

Manganite junction was fabricated by growing a manganite film on the 0.05 wt % Nb-doped $SrTiO_3$ substrate (STON) using the pulsed laser ablation technique. The substrate temperature was kept at 720 °C, and the oxygen pressure was kept at 80 Pa during the deposition. The film thickness was controlled by deposition time. Two series junctions, composed of the $La_{0.67}Ca_{0.33}MnO_3$ (LCMO) films with $t=5-300$ nm and the $La_{0.67}Sr_{0.33}MnO_3$ (LSMO) films with $t=5-200$ nm, respectively, have been prepared.

The junction area is 1×1 mm^2, patterned by the conventional photolithographic and chemical etching technique. Two Cu electrodes were deposited, respectively, on the manganite film and the STON substrate. The electric contacts are Ohmic with the contact resistance of ~15 Ω between Cu and STON and ~200 Ω between Cu and LCMO and LSMO at the ambient temperature. The current-voltage characteristics were measured by a superconducting quantum interference device magnetometer equipped with a resistance measurement unit. The bias voltage that drives the current from LCMO(LSMO) to STON is defined as positive.

The crystal structure of the manganite film was analyzed by the x-ray diffraction technique. The lattice parameter c (out-of-plane) of the LCMO films is present in Fig. 1(a) as a function of film thickness.[8] It exhibits a rapid growth from ~0.3777 to ~0.3805 nm as t increases from ~0 to ~80 nm. The data for $t\rightarrow0$ were obtained based on the Poisson formula $c=V_0/0.3905$ nm volume of the unit cell will remain constant for small lattice distortions assuming the in-plane lattice constant of 0.3905 nm for the LCMO film, where $V_0\approx0.0576$ nm^3 is the unit-cell volume of bulk LCMO. The increase in c with t indicates the presence of considerable tensile strains in the films, the relaxation of which causes the out-of-plane lattice expansion. The most rapid lattice relaxation occurs below the thickness of ~80 nm. The diffraction peaks of LSMO are, unfortunately,

[a]Author to whom correspondence should be addressed. Electronic mail: jrsun@g203.iphy.ac.cn.

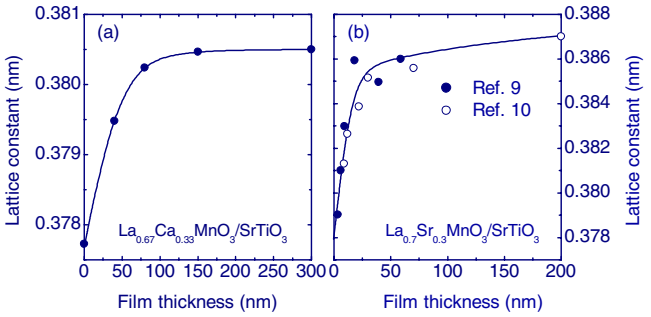

FIG. 1. (Color online) Out-of-plane lattice constant as a function of the thickness of the LCMO films (a) and the LSMO films (b). Solid lines are guides for the eyes.

submerged by those of the substrate. As an alternative, the lattice constants of $La_{0.7}Sr_{0.3}MnO_3/SrTiO_3$, which may share the common features of the LSMO films, are extracted from the literature and presented in Fig. 1(b).[9,10] Similar behavior to that of $LCMO/SrTiO_3$ is observed.

All of the junctions exhibit excellent rectifying behaviors even the ones composed of ultrathin films (Fig. 2). A further analysis reveals a systematic variation in the *I-V* relations with film thickness. As shown in the inset plot in Fig. 2(b), the log *I-V* slope is independent of temperature, when film thickness is 10 nm, or increases with reciprocal temperature, when film thickness is 80 nm. These features are observed in both the LSMO/STON and the LCMO/STON (not shown here) junctions and indicate an evolution of electronic process with film thickness. According to the semiconductor theory, parallel log *I-V* curves suggest the prevalence of electron tunneling in the junctions,[11] while the reciprocal temperature dependence signifies a thermionic emission process.[12]

It is obvious that interfacial potential is the key factor affecting the physical properties of the junctions. The thorough knowledge about it is therefore highly desired, especially for the junctions comprised by the materials that exhibit the characters of strong electron correlation and spin,

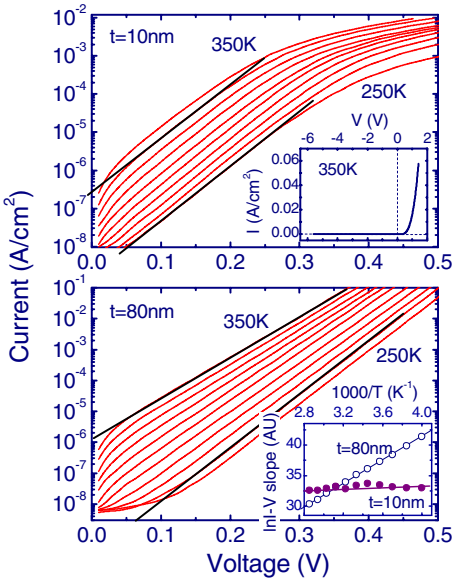

FIG. 2. (Color online) Semilogarithmic plot of the characteristics of the LSMO/STON junction with the film thickness of 10 nm (a) and 80 nm (b). Inset plot in (a): *I-V* curve of LSMO(10 nm)/STON collected at 350 K. Inset plot in (b): log *I-V* slope of the forward *I-V* curves. Solid lines are guides for the eyes.

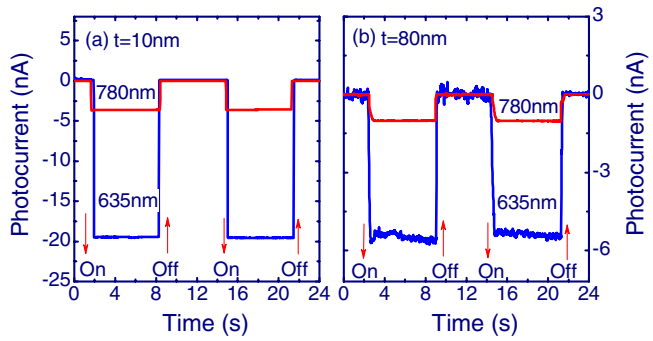

FIG. 3. (Color online) Selected photocurrent of the LCMO/STON junctions for $t=10$ nm (a) and $t=80$ nm (b) measured under the light power of 140 μW and different wavelengths. Arrows signify the positions of light and/or light off.

charge, and orbital coupling. Because of the deviation of the *I-V* relations from the thermionic emission, the interfacial barrier in the junctions composed by ultrathin films (tens of unit cells in thickness) has not been studied before. As is well known, electrons in the LSMO/LCMO electrode can be excited by a light with the energy of $h\nu$ (ν is light frequency), and the hot electrons can penetrate through the junction region under the driving of the built-in electric field when the condition $\Phi_B \leq h\nu \leq E_g$ is satisfied, yielding a photocurrent across the junction, where Φ_B is the Schottky barrier and $E_g \approx 3.2$ eV, is the band gap of $SrTiO_3$. According to Fowler,[13] there is a simple relation between photoresponse (photocurrent per photon, R) and photon energy $R \propto (h\nu - \Phi_B)^2$ when $|h\nu - \Phi_B| \geq 3k_BT$. Based on this relation the interfacial barrier can be experimentally determined. This is an approach that avoids the difficulty to deduce Φ_B from the *I-V* characteristics that deviate from the thermionic emission process.

The laser with the wavelength between 450 and 1000 nm was used in the present experiments. The spot size of the incident light is ~1 mm in diameter. Photocurrent is measured by a Keithley SourceMeter 2601. As a representative, in Fig. 3 we show the photocurrent measured under the lights of 635 and 780 nm for the junctions with $t=10$ and 80 nm. Two distinctive features can be identified. At first, for an identical junction, the light with a shorter wavelength yields a stronger photoresponse. For example, photocurrents are ~19.5 and ~3.8 nA for the wavelengths of 635 and 780 nm (light power=140 μW), respectively, for sample LCMO(10 nm)/STON. Second, photocurrent weakens while film thick-

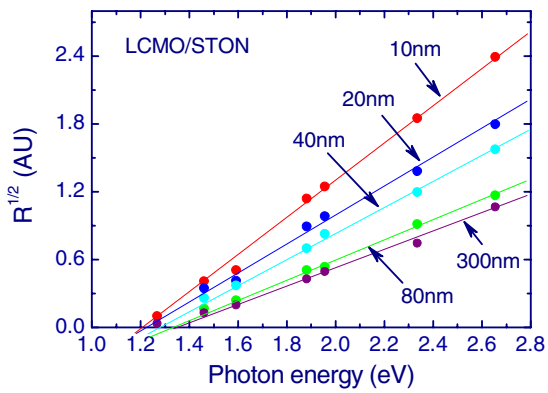

FIG. 4. (Color online) Square root photoresponse as a function of photon energy obtained for the LCMO/STON junctions with different film thicknesses. Solid lines are guides for the eyes.

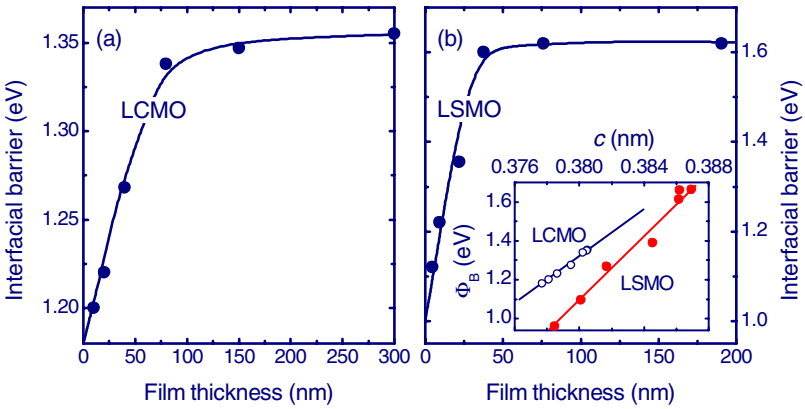

FIG. 5. (Color online) Interfacial barrier as a function of film thickness for the junctions LCMO/STON (a) and LSMO/STON (b). Inset plot: relation between interfacial barrier and out-of-plane lattice constant. Solid lines are guides for the eyes.

ness increases if light parameters are fixed. For example, the photocurrent, under the light of 635 nm, decreases from ~19.5 to ~5.3 nA as t grows from 10 to 80 nm. The former manifests the presence of interfacial barrier, only the light with the energy well above Φ_B is effective, and the latter suggests a change in this barrier with film thickness.

Figure 4 presents the square root of photoresponse as a function of photon energy. Satisfactory linear $R^{1/2}-h\nu$ relations are observed for all samples, indicating the presence of definite interfacial barriers in the junctions. With the growth of film thickness, the $R^{1/2}-h\nu$ slope decreases, accompanying with a high energy shift of the intersection of the $R^{1/2}-h\nu$ curve with the energy axis. The Schottky barrier deduced from the formula given by Fowler is shown in Fig. 5. A remarkable observation is its strong film thickness dependence. For the LCMO/STON junction, for example, Φ_B grows rapidly from ~1.2 to ~1.35 eV as t increases from 10 to 80 nm, with a total change of $\Delta\Phi_B \approx 0.15$ eV. The LSMO/STON junctions share the same features with LCMO/STON except for a much greater increase in Φ_B ($\Delta\Phi_B \approx 0.5$ eV). The relative change in Φ_B is ~13% for LCMO/STON and ~45% for LSMO/STON.

The distinctive dependence of the interfacial potential on film thickness reminds us of lattice constant. It is fascinating that Φ_B and c exhibit similar behaviors against t, as demonstrated by the data in Figs. 1 and 5. The two quantities display a synchronic variation; the former alters only when the latter does. These results imply a strong correlation between Φ_B and c. A direct analysis reveals a simple relation between Φ_B and c: the former grows linearly with the increase of the latter at the rate of ~60.2 eV/nm (LCMO/ASTON) or ~82.1 eV/nm (LSMO/STON) [inset plot in Fig. 5(a)]. Noting the fact that the development of the out-of-plane lattice constant is a signature of in-plane lattice relaxation, this result actually suggests the presence of a close relation between lattice strain and interfacial barrier.

The variation in Φ_B with t conflicts with our knowledge that the Schottky barrier is solely determined by interfacial layers. There are two possible reasons for the strain dependence of the interfacial barrier. The first one is the strain-induced localization of charge carriers. As well established, tensile lattice strains could cause Jahn–Teller-like lattice distortions and high density of defects.[14] Both will enhance the carrier trapping in the films, thus the reduction in Φ_B. The second one is the variation in the electronic state of manganites due to the preferred occupancy of particular orbital when lattice strains exist. It has recently been reported that electrons prefer to occupy the $d_{x^2-y^2}$ orbital in the LSMO films grown on the $SrTiO_3$ substrates.[6] Although it is still not clear how and to what extent this process will affect Φ_B, its influence on Φ_B is anticipated.

The significant reduction in interfacial barrier as film thickness decreases is a feature unaddressed before. It clearly reveals the difference between the interfacial states of the junctions respectively formed by thin and thick layers. This result could be important for the designing of artificial heterostructures. The present work also revealed the difference between the manganites and the conventional semiconductors. The strong coupling between spin/charge/orbital degrees of freedom and lattice strains assigns the manganites distinctive features that emerge only under special conditions. Further study that gives a direct mapping of the interfacial state in the junctions with different film thickness is required, which may be helpful for a thorough understanding of underlying physics.

This work has been supported by the National Natural Science Foundation of China, the National Fundamental Research of China, and the Knowledge Innovation Project of the Chinese Academy of Sciences.

[1]M. Sugiura, K. Uragou, M. Noda, M. Tachiki, and T. Kobayashi, Jpn. J. Appl. Phys., Part 1 **38**, 2675 (1999).
[2]H. Tanaka, J. Zhang, and T. Kawai, Phys. Rev. Lett. **88**, 027204 (2001).
[3]J. R. Sun, C. M. Xiong, T. Y. Zhao, S. Y. Zhang, Y. F. Chen, and B. G. Shen, Appl. Phys. Lett. **84**, 1528 (2004).
[4]J. R. Sun, B. G. Shen, Z. G. Sheng, and Y. P. Sun, Appl. Phys. Lett. **85**, 3375 (2004); Z. G. Sheng, B. C. Zhao, W. H. Song, Y. P. Sun, J. R. Sun, and B. G. Shen, *ibid.* **87**, 242501 (2005).
[5]*Colossal Magnetoresistive Oxides*, edited by Y. Tokura (Gordon and Breach, London, 1999).
[6]M. Huijben, L. W. Martin, Y.-H. Chu, M. B. Holcomb, P. Yu, G. Rijnders, D. H. A. Blank, and R. Ramesh, Phys. Rev. B **78**, 094413 (2008); Y. Tokura and N. Nagaosa, Science **288**, 462 (2000).
[7]Y. Z. Chen, J. R. Sun, S. Liang, W. M. Lu, and B. G. Shen, J. Appl. Phys. **104**, 113913 (2008).
[8]The LCMO compound is of *Pnma* symmetry, and its lattice parameters are $a=0.5457$ nm, $b=0.7711$ nm, and $c=0.5472$ nm. The lattice constants of $a/\sqrt{2}$, $b/2$, and $c/\sqrt{2}$, the ones for idealized perovskite structure, were used here. The in-plane lattice constant of LCMO will be that of $SrTiO_3$ (0.3905 nm) as $t\rightarrow 0$.
[9]P. Orgiani, A. Yu. Petrov, C. Adamo, C. Aruta, C. Barone, G. M. De Luca, A. Galdi, M. Polichetti, D. Zola, and L. Maritato, Phys. Rev. B **74**, 134419 (2006).
[10]S. Jin, G. Gao, W. Wu, and X. Zhou, J. Phys. D **40**, 305 (2007).
[11]P. C. Newman, Electron. Lett. **1**, 265 (1965).
[12]M. Sze, *Physics of Semiconductor Devices*, 2nd ed. (Wiley, New York, 1981).
[13]R. H. Fowler, Phys. Rev. **38**, 45 (1931).
[14]M. Bibes, S. Valencia, L. Balcells, B. Martínez, J. Fontcuberta, M. Wojcik, S. Nadolski, and E. Jedryka, Phys. Rev. B **66**, 134416 (2002).